

# Data analysis and data needs for beryllium-hydrogen charge exchange in tokamak plasmas

P.A. SDVIZHENSKI<sup>1</sup>, V.S. LISITSA<sup>1,2</sup>, A.B. KUKUSHKIN<sup>1,2</sup>, S.N. TUGARINOV<sup>3</sup>

<sup>1</sup>National Research Center “Kurchatov Institute”, Moscow, Russia

<sup>2</sup>National Research Nuclear University MEPhI, Moscow, Russia

<sup>3</sup>Project Center ITER, Moscow, Russia

**ABSTRACT:** The data for the cross-section and kinetic rate of the charge exchange (CX) between beryllium bare nucleus, Be(+4), and hydrogen isotope neutral atom is of great interest for visible-range high-resolution spectroscopy in ITER tokamak because of beryllium first wall in the main chamber. Here an analysis of available data and formulation of data needs are presented. Besides active signal produced by the CX of diagnostic hydrogen neutral beam with impurity ions in plasma, passive signal produced by the CX of impurity ions with cold edge plasma is also important, as it follows from available observation data from JET tokamak with ITER-like beryllium wall. The lack of data in the range of few eV/amu to ~100 eV/amu is shown, especially for data resolved in orbital quantum numbers, which are needed for simulations of level populations of the emitting beryllium ions Be(+3) with the help of two-dimensional, in principal and orbital quantum numbers, kinetic codes.

## 1. INTRODUCTION

The use of beryllium as the material of the first wall in the main chamber of the ITER tokamak requires detailed data for cross sections of elementary atomic processes involving beryllium. Although such processes have been studied in detail, there are still types of processes for which the databases are not complete enough in parameters ranges of interest. Such a process is the charge exchange of bare beryllium ions with hydrogen ions and its isotopes, which plays an important role for optical diagnostics of plasma in the visible spectral range. The charge exchange process can be written in the following general form:



It plays an important role for the Charge eXchange Recombination Spectroscopy (CXRS) diagnostics that Russia will supply to the ITER [1], as well as for other diagnostics of the Active Beam Spectroscopy type as a process that strongly affects the background signal (for more information, see e.g. [2]). For such diagnostics, a diagnostic beam of neutral atoms is injected into the plasma. The plasma ion  $A^{z+}$  interacts with a neutral atom  $B^0$  in the state with the main quantum number  $n_B$  from the diagnostic beam and captures an electron from it. Usually, an electron is captured in the excited state  $A^{(z-1)+}(n, l)$ , where  $n, l$  are the principal and orbital quantum numbers, respectively. The excitation relaxes by emission of radiation, which is collected by the optical system and delivered to the spectrometers.

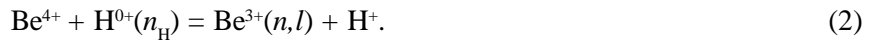
Radiation collected along the line of sight contains the following components:

- active charge exchange lines (charge exchange with a diagnostic beam of hydrogen atoms);
- passive charge exchange lines (charge exchange with hydrogen atoms in the edge plasma);
- passive radiation lines from edge plasma resulting from the excitation of ions and atoms by electron impact;
- continuum radiation.

The CXRS diagnostics measures important plasma parameters such as the concentration and distribution of impurities, ion temperature and plasma rotation rates profiles. A reliable interpretation of the measurements requires predictive modeling of the plasma emission spectra, which, in particular, requires information on the cross sections for the charge exchange reaction (1).

Besides active signal produced by the CX of diagnostic hydrogen neutral beam with impurity ions in plasma, passive signal produced by the CX of impurity ions with cold edge plasma is also important, as it follows from available observation data from JET tokamak with ITER-like beryllium wall (see, e.g., comments and references in [2]).

This paper presents a brief review of the data available in the literature and in databases on cross sections of the charge exchange reaction of bare beryllium nuclei with hydrogen isotopes:



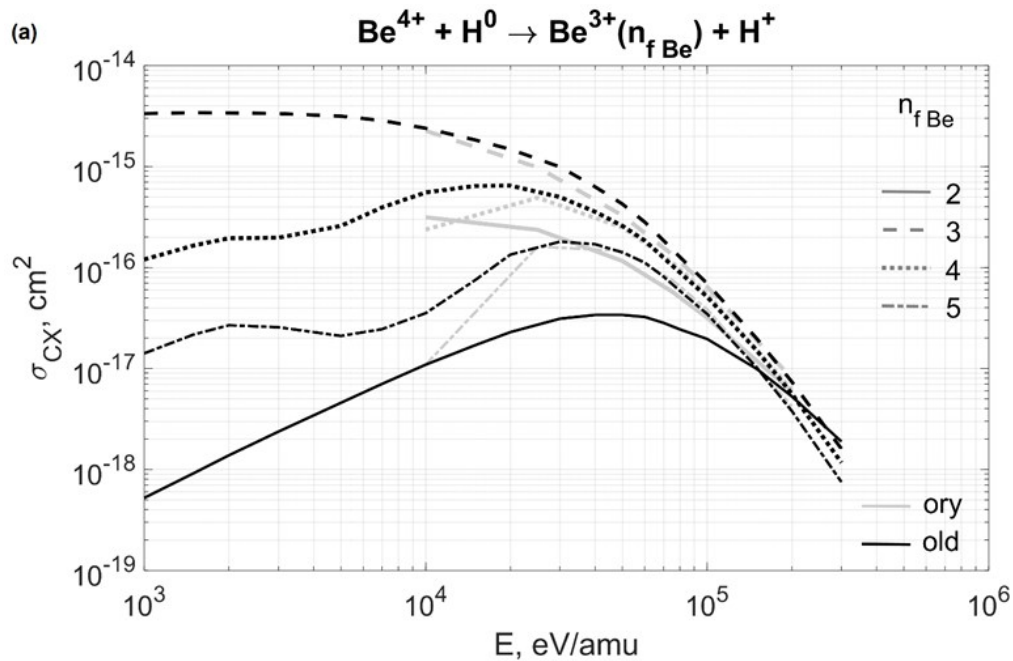
Here the quantum numbers of the state of an atom or ion are indicated in parentheses.

The following transitions of the hydrogen-like beryllium ion Be IV will be used to implement CXRS diagnostics on ITER: 4658.42 Å (6—5 transition) and 4685.4 Å (8—6 transition). Therefore, it is important to have data for charge exchange cross sections at high levels that contribute to the spectral transitions used for measurements.

## 2. REVIEW OF THE AVAILABLE DATA

The figures in this section show the data for cross sections of reaction (2), taken from various sources, as a functions depending on the relative velocity  $v$  and on the collision energy  $E$ , expressed in units of eV/amu. Collision energy  $E = 2.5$  eV/amu corresponds to the relative velocity of colliding particles  $v \approx 0.01$  a.u. ( $\approx 2.188 \cdot 10^4$  m/s); collision energy  $E = 1$  keV/amu corresponds to  $v \approx 0.2$  a.u.

Figure 1 presents a comparison of the data from the OPEN-ADAS database [3, 4] and from [5] on the charge exchange cross sections for hydrogen in the ground state.



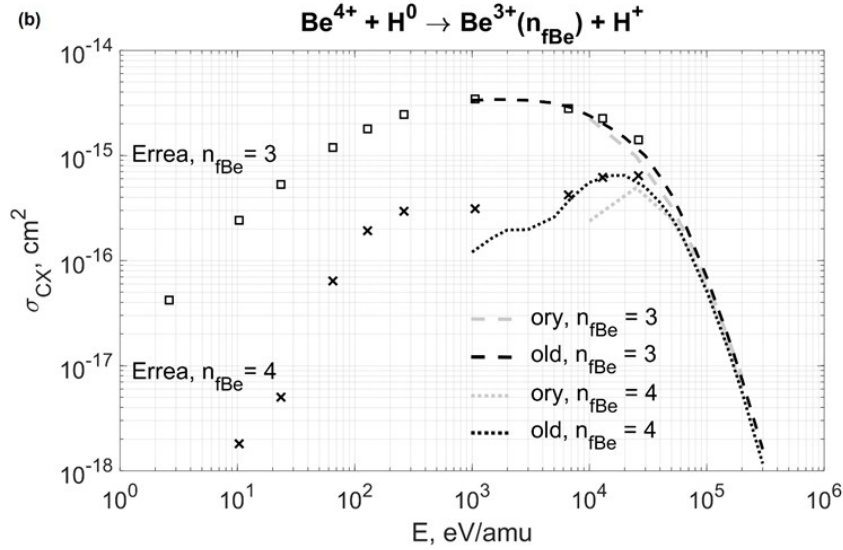


**Figure 1.** The cross sections [3-5] for reaction (2)  $\text{Be}^{4+} + \text{H}^0(n_{iH}=1) = \text{Be}^{3+}(n_{fBe}) + \text{H}^+$ , values of  $n_{fBe}$  are shown in the legend: (a) the data from the OPEN-ADAS database [3, 4]; (b) the comparison of the data from the OPEN-ADAS database [3, 4] and from [5].

The names of the curves (“ory” and “old”) in the legend of Figure 1 refer to the file name from OPEN-ADAS [3, 4] from which the data was taken. The files in OPEN-ADAS have such names as qcx#h0\_#be4.dat, where instead of \* there are the words specified in the legend. Thus, if the curve is labeled “ory” in the legend, this means that it is plotted from the data from the qcx#h0\_ory#c6.dat file. The squares (for populating at the level of  $n_{fBe} = 3$ ) and x markers (for populating at the level of  $n_{fBe} = 4$ ) show the data from *Errea 1998* [5], where information on cross sections at low energies is available.

From Figure 1 one can see that the data available in OPEN-ADAS cover the region of medium and high collision energies, whereas the data for low energies are not available.

Figure 2 presents a comparison of the data from the OPEN-ADAS database for charge exchange cross sections for hydrogen in the ground and excited states.

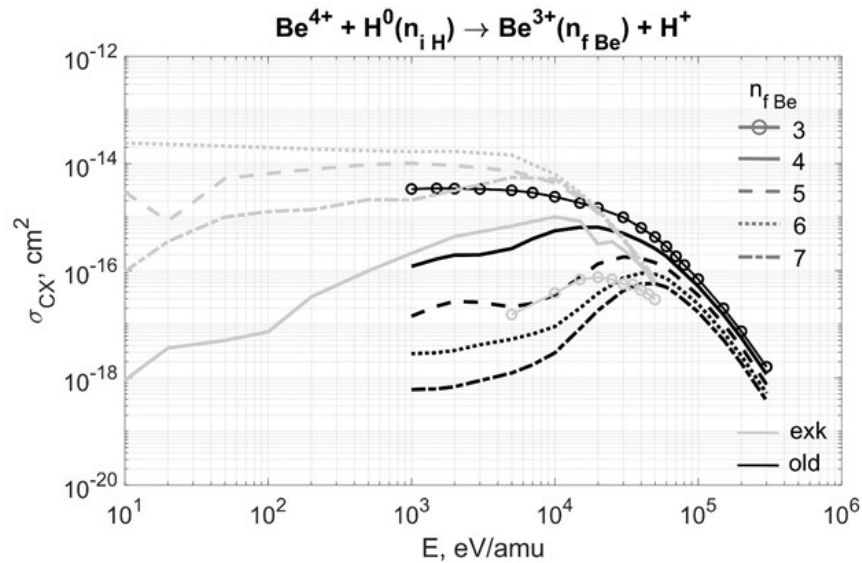


**Figure 2.** The comparison of cross sections [3, 4] for reaction (2) for  $n_{iH} = 1$  (black curves) and for  $n_{iH} = 2$  (gray curves), i.e. in the latter case, charge exchange occurs with hydrogen in the excited state. Other notations are the same as in Figure 1.

Figure 2 shows that the charge exchange cross sections for hydrogen in the excited state are higher than those for hydrogen in the ground state. In the first case, the largest cross section corresponds to the charge exchange with populating the level with the principal quantum number  $n = 6$ , in the second – the level  $n = 3$ .

Figures 3 and 4 below show the data from the qcx#h0\_en2\_kvi#be4.dat file from OPEN-ADAS for charge exchange with excited hydrogen  $\text{Be}^{+4} + \text{H}^0(n_{\text{H}}) = \text{Be}^{+3}(n_{\text{fBe}}, l) + \text{H}^+$  with populating the levels with different  $n_{\text{fBe}}$  and  $l$ .

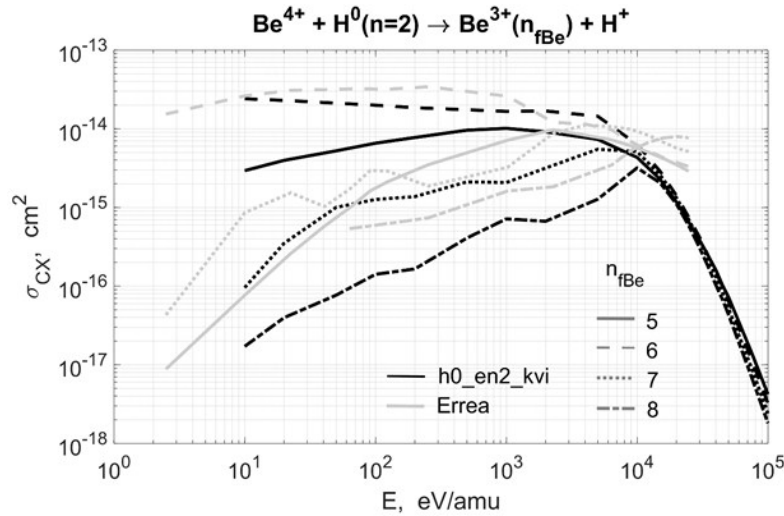


Figure 3. The charge exchange cross sections for reaction (2), according to the data from the qcx#h0\_en2\_kvi#be4.dat file [3, 4] (black curves) and data from [5] (gray curves).

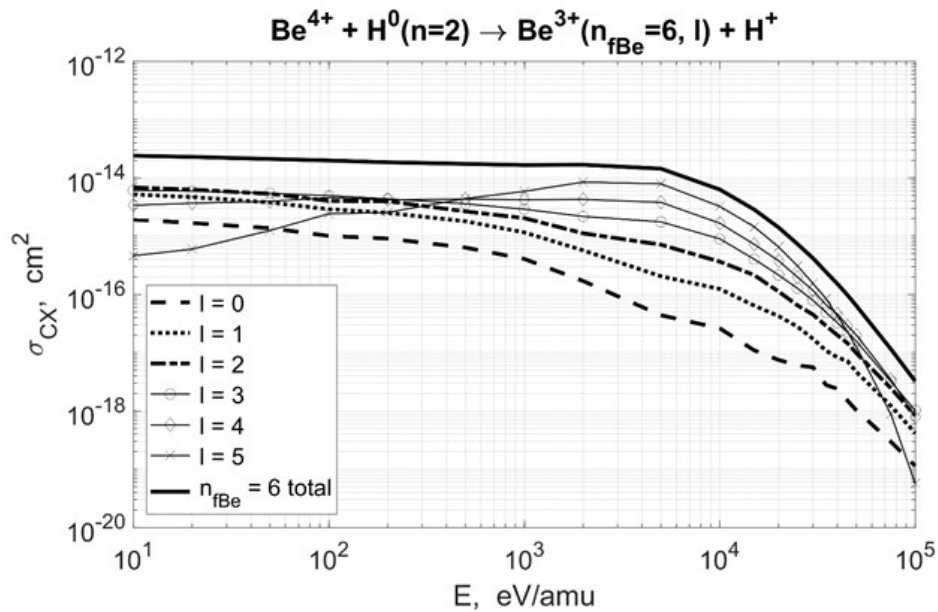


Figure 4. The charge exchange cross sections for reaction (2), according to the data from qcx#h0\_en2\_kvi#be4.dat file [3, 4] for populating the levels with  $n_{\text{fBe}} = 6$  and different  $l$ .

### Comparison of cross sections from Errea 1996 [6] and Janev 1996 [7]

Figures 5—8 below show the comparison of charge exchange cross sections for reaction (2), taken from *Errea 1996* [6] and *Janev 1996* [7]. Figure 9 shows the dependence of charge exchange cross sections for reaction (2) on orbital quantum number  $l$  for different values of principal quantum number  $n$ .

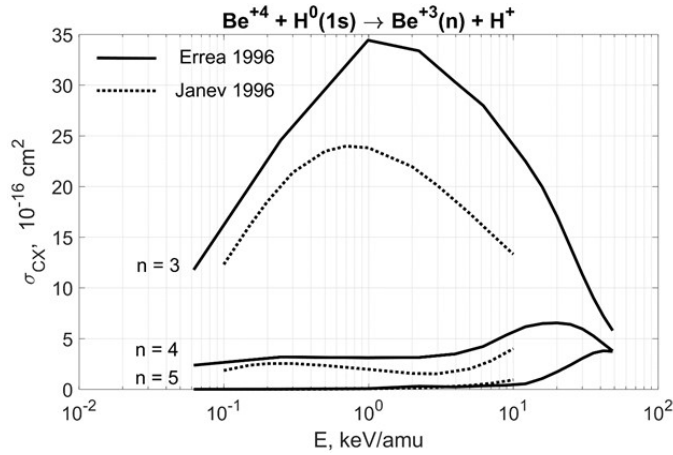


Figure 5. Total charge exchange cross sections for reaction (2) for electron capture to the state with principal quantum number  $n$  (the values of  $n$  are shown in the figure). Solid curves – data from *Errea 1996* [6], dotted curves – data from *Janev 1996* [7].

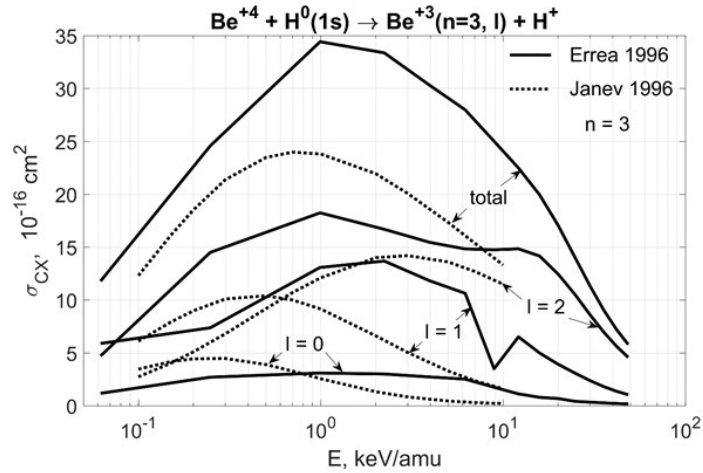


Figure 6. Partial charge exchange cross sections for reaction (2) for electron capture to the state with principal quantum number  $n = 3$  and orbital quantum number  $l$  (the values of  $l$  are shown in the figure). Solid curves – data from *Errea 1996* [6], dotted curves – data from *Janev 1996* [7].

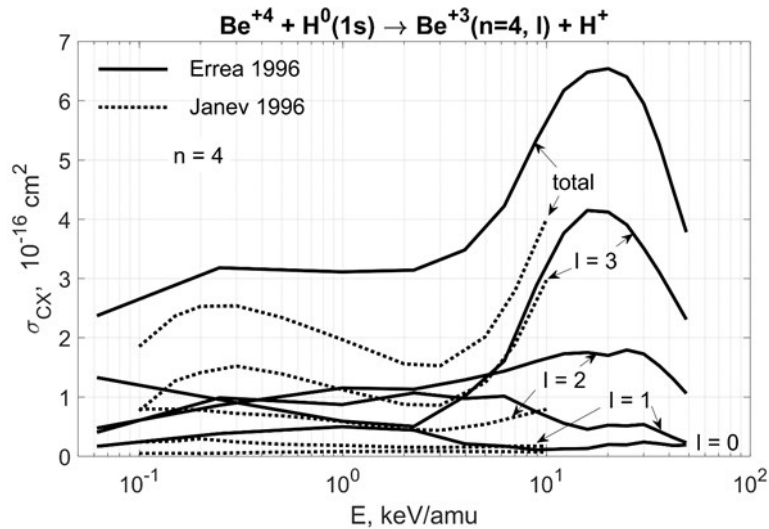


Figure 7. Same as in Figure 6, but for  $n = 4$ .

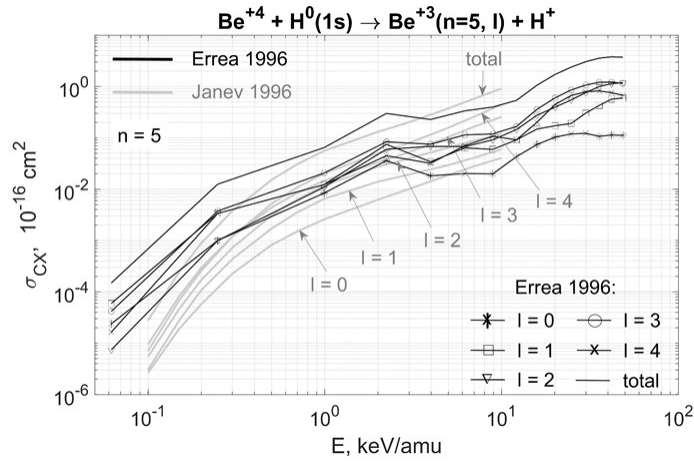


Figure 8. Same as in Figure 6, but for  $n = 5$ .

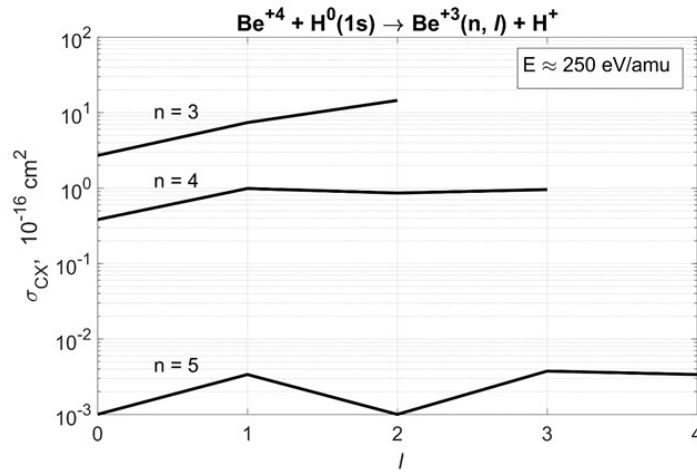


Figure 9. The dependence of charge exchange cross sections for reaction (2) on orbital quantum number  $l$  for different values of  $n$  (the values of  $n$  are shown in the figure). The data from *Errea 1996* [6] are used.

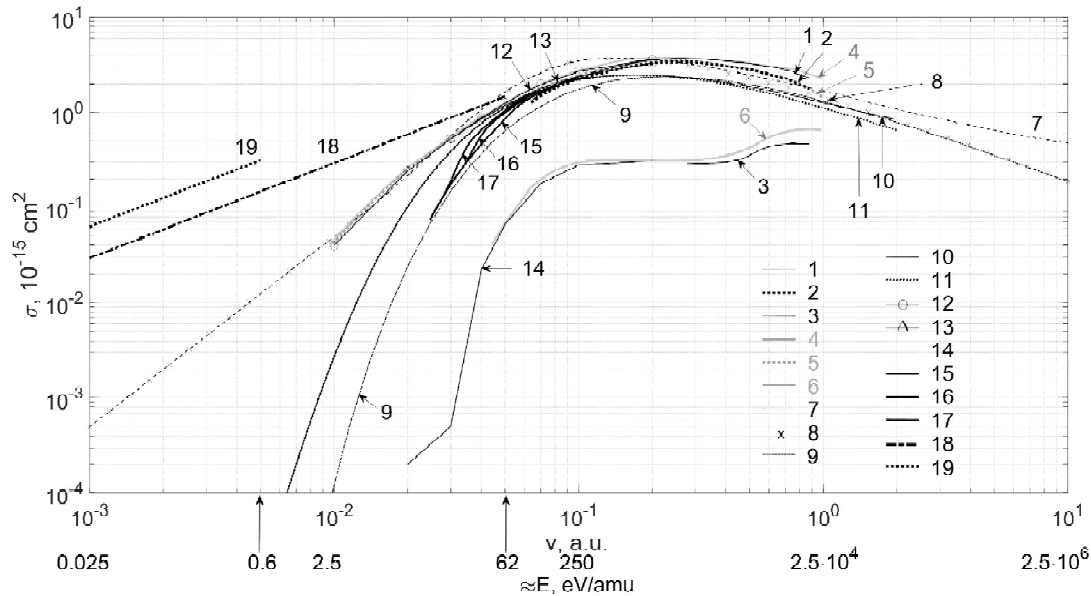


Figure 10. A survey of data for cross sections for reaction (2). The sources of data are indicated in the legend. The notations of curves are explained in the text below.

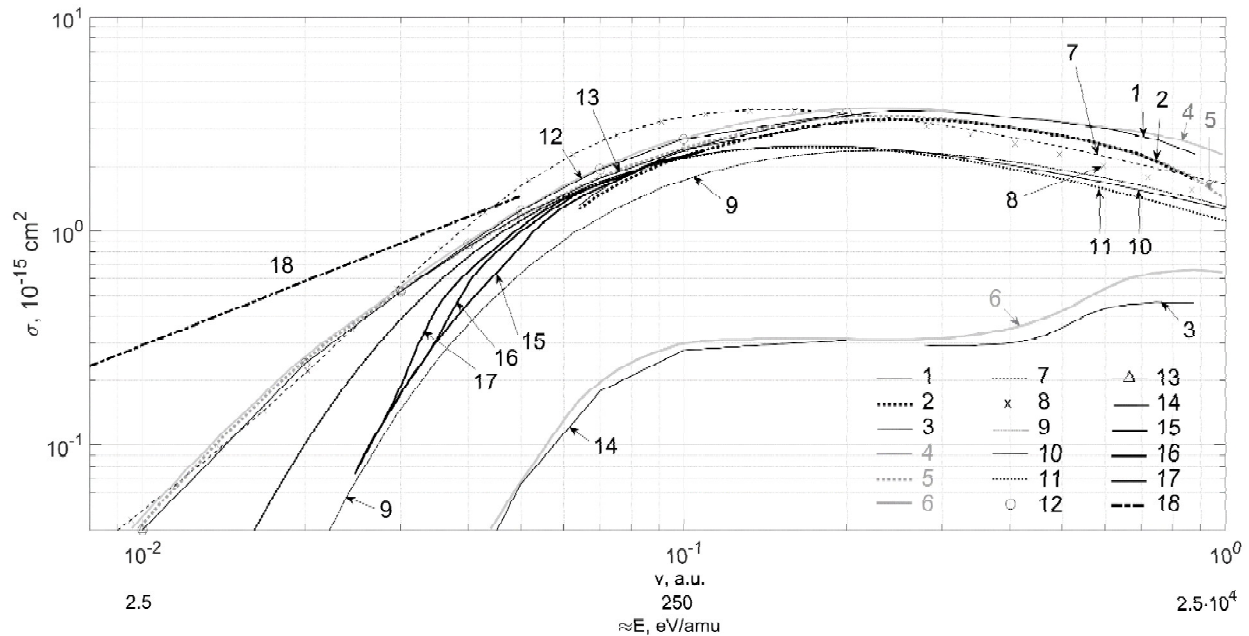


Figure 11. An enlarged fragment of Figure 10.

From Figures 5–8 one can see that in the range of collision energies below 100 eV/amu there is practically no data resolved in orbital quantum numbers  $l$ .

Figures 10 and 11 shows a comparison of the charge exchange cross sections calculated by various methods for reaction (2), taken from various sources.

The notations of the curves in Figures 10 and 11 are as follows. The curves 1, 2, and 3 stand for the calculation [8] of the total cross section and partial cross sections for  $n = 3$  and  $n = 4$ , respectively, using 21-state atomic-orbital expansion. The curves 4, 5 and 6 stand for the calculation [5] of the total cross section and partial cross sections for  $n = 3$  and  $n = 4$ , respectively, using molecular expansion with semiclassical and quantal calculations for 96- and 17-state basis sets. The curves 7 and 8 stand for our calculations of the total cross section and partial cross section for  $n = 3$ , respectively, in the frame of Landau-Zener model with rotation taken into account [9], while curve 9 is the same but without rotation taken into account [9]. The curves 10 and 11 stand for the total cross section and partial cross section for  $n = 3$ , respectively, according to the Kronos database [10]; the model is described in [11]. The curves 12, 13, and 14 stand for the calculation [12] of the total cross section and partial cross sections for  $n = 3$  and  $n = 4$ , respectively, using the hyperspherical close-coupling (HSCC) approach. The curve 15 stands for calculation [13] for hydrogen; the curve 16 stands for calculation [13] for **deuterium**  $\text{Be}^{4+} + \text{D}(1s) \rightarrow \text{Be}^{3+}(n) + \text{D}^+$  (for more details on the isotopic effect see, e.g., [14] or review [15]); the curve 17 stands for calculation [13] for **tritium**:  $\text{Be}^{4+} + \text{T}(1s) \rightarrow \text{Be}^{3+}(n) + \text{T}^+$ ; calculations were performed in the frame of the adiabatic theory of transitions in slow collisions using the ARSENY code, based on the hidden crossings method. The curve 18 stands for low velocities asymptotic (2.18) in [9] with  $|b_+(R)/b_-(R)| = 1$ ,  $n = 3$ ,  $Z = 4$ ,  $R_0 = R_{n=3}$ , where  $R_n$  is defined by (2.2) in [9]; the curve 19 stands for low velocities asymptotic (2.19) in [9] with , , where  $R_n$  is defined by (2.2) in [9],  $V$  is defined by (1.1) in [9].

In the lack of experimental data, special attention must be paid to the accuracy and reliability of the calculations. The most reliable are the results obtained using the atomic/molecular orbital method, or their variations. One of the drawbacks of calculations using the Landau-Zener model is the impossibility of calculating the charge exchange cross sections with populating the levels with the principal quantum number  $n \geq Z$ , where  $Z$  is the ion charge.

It can be seen from this section that in the literature and in existing databases (e.g., OPEN-ADAS [3, 4]), most of the available information on the charge exchange cross sections covers the range of energies that are of interest primarily for calculating the active signal, i.e. for diagnostic beams with energies of tens and hundreds of keV. At the

same time, for estimations of the passive charge exchange signal (see, e.g., recently suggested algorithm [16]), when the energy of neutral atoms coming from the wall is in the range from few eV to tens or hundred of eV, the data is not enough, especially for *l*-resolved data. Therefore, additional theoretical calculations of the cross sections may be necessary for the charge exchange reactions of interest, which are needed for simulations of level populations of the emitting beryllium ions Be(+3) with the help of two-dimensional, in principal and orbital quantum numbers, kinetic codes like the *nl*-KINRYD code [17].

### 3. CONCLUSIONS

A brief analysis of the available data on the cross sections of the charge exchange reaction of bare beryllium nuclei on hydrogen isotopes is carried out. It is shown that there is a lack of data in the region of low (below 100 eV/amu) collision energies, which is of interest for modeling a passive CXRS diagnostic signal in ITER.

### ACKNOWLEDGEMENTS

The authors are grateful to M. G. O'Mullane for discussing the subject of this paper, and I. Yu. Tolstikhina for discussing this paper.

### References

- [1]. Tugarinov S.N., *et al*, 2004 Plasma Physics Reports 30, No 2, 128-135.
- [2]. Von Hellermann M.G., *et al*, 2019 Atoms 7, No 1, 30. <https://doi.org/10.3390/atoms7010030>
- [3]. OPEN-ADAS (Atomic Data and Analysis Structure), <http://open.adas.ac.uk/>
- [4]. Summers H. P., O'Mullane M. G. Atomic data and modelling for fusion: The ADAS Project. *AIP Conf. Proc. ATOMIC AND MOLECULAR DATA AND THEIR APPLICATIONS: 7th International Conference on Atomic and Molecular Data and Their Applications (ICAMDATA-2010)*, 1344:179–187, 2011. (doi:10.1063/1.3585817)
- [5]. Errea L.F. *et al* 1998 J. Phys. B: At. Mol. Opt. Phys. 31 3527.
- [6]. Errea L.F. *et al*. 1996 Phys. Scr. T62, 27.
- [7]. Janev R.K. *et al*. 1996 Phys. Scr. T62, 43.
- [8]. Fritsch W., Lin C. D., 1984 Phys. Rev. A 29, 3039.
- [9]. Abramov V.A., Baryshnikov F.F., Lisitsa V.S. 1978 Sov. Phys. JETP 47(3), 469.
- [10]. Kronos database, <https://www.physast.uga.edu/research/stancil-group/atomic-molecular-databases/kronos>
- [11]. Mullen P. D. *et al*, 2016 The Astrophysical Journal Supplement Series 224, No 2, 31.
- [12]. Le Anh-Thu *et al*. 2003 J. Phys. B: At. Mol. Opt. Phys. 36, 3281.
- [13]. Tolstikhina I.Yu. *et al*. 2014 J. Phys. B: At. Mol. Opt. Phys. 47, 035206.
- [14]. Tolstikhina I.Yu., Tolstikhin O. I., 2015 Phys. Rev. A, 92, 042707.
- [15]. Tolstikhina I.Yu., Shevelko V. P., 2018 Physics-Uspokhi 61, No. 3, 247.
- [16]. Sdvizhenskii P.A., Kukushkin A.B., Levashova M.G., Lisitsa V.S., Neverov V.S., Serov S.V., Tugarinov S.N. Proc. 46th EPS Conference on Plasma Phys., Milan, Italy, 2019, ECA vol. 43C, P4.1006, <http://ocs.ciemat.es/EPS2019ABS/pdf/P4.1006.pdf>
- [17]. Kadomtsev M.B., Levashova M.G., Lisitsa V.S., 2008 JETP 106, 635-649.